

12/18/03

Spectral Absorption of Solar Radiation By Aerosols during ACE-Asia

By

R.W. Bergstrom¹, P. Pilewskie², J. Pommier¹, M. Rabbette¹,
P. B. Russell², B. Schmid¹, J. Redemann¹, A. Higurashi³,
T. Nakajima⁴, P.K. Quinn⁵

¹ Bay Area Environmental Research Institute
560 Third St. West
Sonoma, CA 95476

² NASA Ames Research Center
Moffett Field, CA

³ National Institute of Environmental Studies
Tokyo, Japan

⁴ Center for Climate Systems Research
University of Tokyo

⁵ NOAA Pacific Marine Environmental Laboratory
Seattle, WA

Submitted to the Journal of Geophysical Research
For inclusion in the ACE Asia Special Section part 2

December, 2003

Abstract

As part of the Asian Pacific Regional Aerosol Characterization Experiment (ACE Asia), the upward and downward spectral solar radiant fluxes were measured with the Spectral Solar Flux Radiometer (SSFR) and the aerosol optical depth was measured with the Ames Airborne Tracking Sunphotometer (AATS-14) aboard the CIRPAS Twin Otter aircraft. In this paper we examine the data obtained for two cases; a moderately thick aerosol layer - April 12, and a relatively thin aerosol case - April 16, 2001. On both days, the Twin Otter flew vertical profiles in the Korean Strait southeast of Gosan Island.

For both days, we determine the aerosol spectral absorption of the layer and estimate the spectral aerosol absorption optical depth and single scattering albedo. The results for April 12th show that the single scattering albedo increases with wavelength from 0.8 at 400 nm to 0.95 at 900 nm and remains essentially constant from 950 to 1700 nm. On April 16th the amount of aerosol absorption was very low; however, the aerosol single scattering albedo appears to decrease slightly with wavelength in the visible region. These results are indicative of a mineral dust/black carbon mixture for April 12th and possibly a black carbon/pollution mixture for April 16th. For the April 12th case we attempt to estimate the relative contributions of the black carbon particles and the dust particles.

We compare our results with other estimates of the aerosol properties from a SeaWiFS satellite analysis, aerosol measurements made aboard the Twin Otter, the NOAA Ronald H. Brown ship and ground sites in Gosan and Japan. The results indicate a relatively complicated aerosol mixture of both industrial pollution (including black carbon) and mineral dust. This underscores the need for careful measurements and analysis to separate out the absorption effects of mineral dust and black carbon in the East Asia region.

1. Introduction

The Asian Pacific Regional Aerosol Characterization Experiment (ACE Asia) was carried out during March-May 2001 [Huebert *et al.*, 2003*a,b*]. Its purpose was to investigate the outflow of aerosols from East Asia during the spring months with particular emphasis on mineral dust outbreaks and air pollution transport. The ACE Asia intensive field program consisted of measurements made aboard several aircraft (including a Twin Otter and a C130), the NOAA ship Ronald H. Brown and ground stations at Gosan, Korea and various locations in Japan. Measurements were also made in conjunction with several satellite sensors (*e.g.* SeaWiFS, MODIS, MISER, AVHRR). The study was also coordinated with the APEX program [Nakajima *et al.*, 2003] and the TRACE-P study [Jacob *et al.*, 2003]. For an overview of the ACE Asia study, see Huebert *et al.* [2003*a*].

The initial results of the study have been described in a number of papers (JGR special section, Vol. 108 D23, 2003) that discuss various aspects of the aerosols measured during ACE Asia. During the study period aerosols from pollution sources, biomass burning and mineral dust from the inland Chinese deserts were transported from the interior to the coast of East Asia. Significantly, several outbreaks of mineral dust occurred during March and April, 2001. One of the most important findings of the ACE Asia study is that the aerosol particles off the coast of East Asia were complex mixtures of mineral dust, pollution particles and seasalt. These combinations of particle types are highly variable and make attribution of the aerosol radiative properties to specific aerosol types difficult without detailed measurements.

We report here on the characterization of the solar spectral irradiance fields prevalent during two distinct aerosol cases over the Korean Strait during the ACE Asia study period. The first case on April 12, 2001, was characterized by a moderately thick layer of pollution and dust aerosols while the second case on April 16th had a relatively thin aerosol layer. Net solar irradiance spectra obtained at multiple levels above and below the aerosol layer provided the means to derive the layer absorption spectra. Optical depth spectra were used with the absorption spectra in a radiative transfer model to estimate the spectral absorption optical depth and single scattering albedo. These results are interpreted as to the relative contributions of black carbon and dust particles.

[Note: We use the term "black carbon" to represent all the solar radiation absorbing carbonaceous particles. As pointed out by a number of authors, the term is somewhat ambiguous since it does not differentiate between graphitic-like carbon particles (sometimes called EC for elemental carbon) and amorphous carbon particles. Perhaps a better term is LAC for light absorbing carbonaceous particles, however, we use black carbon in this paper for simplicity.]

2. Radiation Measurements and Modeling

During the ACE Asia intensive field study the NASA Solar Spectral Flux Radiometer (SSFR) was deployed on the CIRPAS Twin Otter to measure upwelling and downwelling solar spectral irradiance. The SSFR-measured irradiance has an absolute uncertainty of 1-3 % over the wavelength range from 300-1700 nm. There is additional error associated with variation in the aircraft pitch and roll. For a description of the instrument, the calibration and a discussion of errors see *Pilewskie et al.* [2003].

The NASA Ames Airborne Tracking 14-channel Sunphotometer (AATS-14) was aboard the Twin Otter to measure the transmission of the direct solar beam in 14 channels (354 to 1558 nm). The data obtained by the AATS-14 are presented in *Schmid et al.*, [2003]. The AATS-14 is an enhanced version of the AATS-6 instrument which flew on the C-130 aircraft during ACE-Asia [*Redemann et al.*, 2003]. The methods for data reduction, calibration, and error analysis have been described previously (see *Schmid et al.* [2003]).

We developed a numerical radiative transfer model specifically for analysis of the SSFR data [*Bergstrom et al.*, 2003]. The major features of the model are the following:

- a. k-distribution representation for O₂, O₃, CO₂ and H₂O absorption coefficients [*Mlawer et al.*, 1997]
- b. DISORT, a multiple scattering code [*Stamnes et al.*, 1988]
- c. Kurucz representation of the solar spectrum [*Kurucz*, 1992]
- d. Filter functions from the SSFR [*Pilewskie et al.*, 2003]

The model contains 140 bands of 10 nm width from 300 to 1700 nm matching the spectral coverage of the SSFR. The inputs are the vertical profiles of the gases, aerosol

and clouds; as well as the spectral scattering and absorption properties of the aerosols and clouds. The spectral surface reflectance and the solar angle are also inputs. We simplify the aerosol scattering by assuming a Henyey-Greenstein phase function. This required specifying only the first moment of the phase function, the asymmetry parameter, g . Further details about the radiative transfer model are in *Bergstrom et al.* [2003].

2.1 Comparison of Measured and Computed Irradiance

Figure 1 shows the measured and calculated downward solar flux at 2 km above the ocean surface for April 12, 2001 and also illustrates the measurements and model spectral resolution. The calculated solar flux spectrum results from the Kurucz solar spectrum attenuated by molecular scattering, aerosol scattering and absorption, O_2 , O_3 absorption in the UV, the O_2 A and B bands centered at 762 nm and 688 nm respectively, the H_2O bands centered at 1380, 1135, and 942 nm as well as several visible H_2O bands, and the CO_2 bands at 1400 and 1600 nm.

2.2 Determining the Aerosol Absorption and Single Scattering Albedo

By measuring the upward and downward solar irradiance (when differenced yield the net solar flux) at two heights in the atmosphere, we can determine the fractional absorption (α) of the layer between the two levels [*Pilewskie et al.*, 2003]:

$$\alpha = \frac{(F_{\downarrow} - F_{\uparrow})_2 - (F_{\downarrow} - F_{\uparrow})_1}{F_{\downarrow 2}}$$

where F_{\downarrow} and F_{\uparrow} are the downward and upward irradiance, respectively, at the lower (subscript 1) and the upper (2) heights.

The relationship of the single scattering albedo, ω (the ratio of scattering to extinction), to the fractional absorption can be written formally as [*Chandrasekhar, 1960*; pg11, equation (56)]

$$\alpha = \int_{\Delta\tau} (1-\omega) \left[\int_{4\pi} I(\tau, \Omega) / F_{\downarrow 2} d\Omega \right] d\tau \quad (1)$$

12/18/03

where I is the intensity (or radiance), Ω is the solid angle and τ is the optical thickness at a particular wavelength.

Equation (1) indicates that the fractional absorption is proportional to the co-albedo $(1-\omega)$. Since the spectral intensity is integrated over all angles, the fractional absorption is only weakly dependent on the scattering distribution function (or asymmetry factor). Therefore, the fractional absorption is a good indicator of the spectral co-albedo.

As shown in *Bergstrom et al.*, [2003] we can express the error in the single scattering albedo in the limit of single scattering as

$$\delta\omega = (1-\omega) \frac{\delta\alpha}{\alpha} + \frac{(1/\mu_0 e^{-\tau/\mu_0})}{(1 - e^{-\tau/\mu_0})} \delta\tau \quad (2)$$

From Equation 2 we can estimate the uncertainty in the single scattering albedo from the uncertainty in the fractional absorption, α and the uncertainty in the optical depth, τ .

3. Moderately thick aerosol layer - April 12, 2001

On the morning of April 12th, the Twin Otter flew from Iwakuni Marine Corps Air Station (MCAS) on the Island of Honshu near Hiroshima out into the Korean Strait to a location 33°N by 128°W, some 160 km east of the island of Gosan. The NOAA ship Ronald H. Brown was at 35°N by 130°W, about 400 km to the northeast of Gosan. The C130 flew from Iwakuni MCAS into the Yellow Sea making several spirals near Gosan and continuing to the west coast of Korea then north over the Yellow Sea.

The location of the aircraft and Ron Brown for April 12th are shown in Figure 2. (Figure 2 is from the meteorological forecast map issued before the flights on April 12 by Prof. John Merrill of the University of Rhode Island.)

3.1 Atmospheric Conditions on April 12, 2001

The ACE Asia intensive period was marked by transport of pollution from East Asia and several mineral dust outbreaks. The largest dust outbreak occurred on about April 6th in the inland Chinese deserts. Portions of the dust plume moved across the

12/18/03

Pacific north of the Japanese Islands and reached the United States on April 11th [*Jaffe et al.*, 2003; *Thulasiraman et al.*, 2002]. Smaller amounts of the dust were transported south into the ACE Asia region during the period of April 10th - 13th. The dust was widespread for several days including April 12th [*Matusmoto et al.*, 2003b].

The meteorology of April 12th (see Figure 2) shows a low pressure system pulling the aerosol through the Korean Strait region from west to east. The back trajectory analysis indicates that the lower boundary layer air in the Korean Strait came from central Asia and over Korea. The air apparently contained dust particles from the April 6-7 storm and then mixed with industrial pollution aerosol before it reached the Korean Strait.

A SeaWiFS image and aerosol optical depth analysis using the procedure of *Higurashi and Nakajima* [2002] for April 12th are shown in Figures 3a and 3b respectively. The SeaWiFS image shows the haze in the area where the measurements were taken and illustrates the spatial variability of the aerosol on April 12th. The analysis predicts an aerosol optical depth where the Twin Otter was located of about 0.35 at 500 nm. The analysis yields larger aerosol optical depth to the west of the Twin Otter, in particular at Gosan Island where the C130 flew spirals and to the east where the Ron Brown was located on that day.

The Twin Otter made several passes at various altitudes over the location 33°N, 128°W before returning to Iwakuni, MCAS. The flight location and heights for April 12, 2001 are shown in Figure 4. Profiles of the multiwavelength aerosol optical depth and derived extinction coefficients from the AATS-14 aboard the Twin Otter are shown in Figure 5. The analysis performed by *Schmid et al.* [2003] using the AATS-14 extinction spectra indicated three layers - two lower layers (0-1.8 km) and an upper layer above about 2 km. They show that while the upper layer had small particles with a large Angstrom exponent, the total column optical depth was dominated by two lower layers with larger particles. The Angstrom exponent for the optical depth of the entire column was about 0.54 for wavelengths between 450 to 700 nm.

The Twin Otter carried a number of aerosol sampling instruments [*Huebert et al.*, 2003]. *Mader et al.*, [2002] present elemental carbon, total organic carbon and carbonate mass from the aerosol sampling made aboard the Twin Otter. They measured an average

value of elemental carbon of $0.56 \mu\text{gm}/\text{m}^3$ for the April 12th flight. They also show that there appears to have been a significant amount of dust present as suggested by the amount of carbonate.

Quinn et al. [2003] present optical depth and absorption results from measurements made aboard the Ron Brown. For April 12th they show aerosol optical depths of about 0.5 at 500 nm. *Quinn et al.* [2003] report that dust made up $70 \pm 20\%$ of the sub-10 micron aerosol mass during this period and EC made up less than 1%. The AERONET network (<http://aeronet.gsfc.nasa.gov/>) and *Bush et al.* [2003] report aerosol optical depths at Gosan of about 0.3 at 500 nm as does *Redemann et al.* [2003] from AATS-6 aboard the C130.

3.2 Measurements of the Spectral Solar Fluxes and Absorption

The measured fractional atmospheric absorption [Equation (1) above] for the aerosol layer between 43m and 2700m is shown in Figure 6, along with modeled spectra using two different values of the aerosol single scattering albedo. The measured fractional absorption in the layer decreases from greater than 0.1 at 350 nm to 0.04 in the mid-visible and stays relatively low in the region between the gas absorption bands in the near infrared. Comparison of the measured absorption spectrum with the modeled spectra shows that the single scattering albedo must be ~ 0.8 in the near UV and increase with wavelength. That is, the modeled absorption for a single scattering albedo of 0.8 agrees with the measurements at 350 nm and the modeled absorption for a single scattering albedo of 0.99 is fairly close to the measurements at wavelengths longer than about 650 nm.

The most prominent features in the absorption spectrum are the gas absorption bands. The water vapor bands centered at 942, 1135 and 1380 nm cause large peaks in the spectra. Retrieving the aerosol absorption is most reliable in the regions away from the gas absorption bands. In particular the regions of 350 - 700 nm, 800 - 900 nm, 1000 - 1100 nm, 1200 - 1300 nm and 1500 - 1600 nm are regions least influenced by gaseous absorption.

3.3 Estimates of the Spectral Single Scattering Albedo and Absorption Optical Depth

The single scattering albedo $\omega(\lambda)$ for the layer can be derived from the measured fractional absorption $\alpha(\lambda)$ and the optical depth $\tau(\lambda)$ by interpolating the model results at each λ to make the model $\alpha(\lambda)$ equal the measured $\alpha(\lambda)$. The single scattering albedo result for April 12 is shown in Figure 7.

The derived single scattering albedo has a minimum in the UV at 0.80 and increases through the visible to a relatively constant value of 0.95. Although there was considerable black carbon in the atmosphere sampled on this flight [Mader *et al.*, 2002] the wavelength dependence of the single scattering albedo does not have a typical black carbon wavelength dependence [Bergstrom *et al.*, 2002; 2003, Dubovik *et al.*, 2002]. The wavelength dependence in Figure 7 is similar to a mineral dust single scattering albedo [Dubovik *et al.*, 2002; Sokolik and Toon, 2002]. The values for Persian Gulf desert dust from Dubovik *et al.* [2002] are shown in Figure 7 for comparison. While the spectral shape is similar, the derived values are slightly lower than the Dubovik *et al.* [2002] values.

To understand the spectral behavior of the single scattering albedo, we plot the aerosol extinction optical depth and absorption optical depth for April 12 in Figure 8. The wavelength dependence of the single scattering albedo depends on the wavelength dependence of both the extinction and the absorption ($\omega = 1 - \tau_{\text{abs}}/\tau$). If the extinction optical depth and absorption optical depth are approximated by power laws, *i.e.*

$$\tau \sim \lambda^{-a}; \quad \tau_{\text{abs}} \sim \lambda^{-b} \quad (\text{where } \tau \gg \tau_{\text{abs}}), \quad (3)$$

then for $a > b$ the single scattering albedo will decrease with wavelength and for $b > a$ the single scattering albedo will increase with wavelength. The curve of the derived single scattering albedo in Figure 7 indicates that for the April 12th case $b > a$. This is shown in Figure 8 where a power law fit to the optical depth is approximately $\lambda^{-0.45}$ while the absorption optical depth falloff is $\lambda^{-2.0}$.

The Angstrom exponent (the quantity a in Equation 3 above) indicates the relative size of the particles. A value of 0.45 for the fit to the optical depth indicates that the particles were fairly large, most likely containing dust particles as reported by Quinn *et al.* [2003]. Additionally, data from Gosan indicate that the dust transported from the

12/18/03

inland deserts reached the surface around 3 UT on April 10 and persisted until about 0 UT on April 14 [*Schmid et al.*, 2003].

It is difficult to tell from just the wavelength dependence of the absorption optical depth in Figure 8 whether the absorption was caused solely by black carbon particles or a combination of dust and black carbon particles. In general most of the spectral absorption results for black carbon particles indicate a power law exponent of 1 to 2, where 1 is the small particle limit for wavelength-independent refractive indices. *Bergstrom et al.* [2002; 2003] found a value of 1 for pollution over the North Atlantic and a value of 1.3 for biomass burning particles in South Africa). However, *Bond et al.* [2002] show that the absorption from carbon particles produced from residential fuel use can have a power law exponent between 1 and 2.9. *Schnaiter et al.* [2003] found that while diesel soot particles have a wavelength dependence of λ^{-1} , spark-gap generated black carbon particles have a wavelength dependent absorption of λ^{-2} . Thus, a wavelength dependence of 2.0 could be caused by black carbon particles alone. (Very recently, *Kline et al.* [2003] reported a wavelength dependence of λ^{-1} for the aerosol absorption from plumes from Asian population centers measured at Amani Ohshima, Japan.)

For the measured black carbon particles to account for all the measured absorption, they would also have to have a relatively high mass absorption coefficient in the mid-visible, approximately 25 m²/gm. A number of ACE Asia investigators (*Chuang et al.*, [2003] at Gosan, *Clarke et al.*, [2003] on the C130, *Anderson et al.*, [2003] on the C130, *Mader et al.*, [2002] on the Twin Otter and *Quinn et al.*, [2003] on the Ron Brown) found a range of the mass absorption coefficient of black carbon particles to be between 5 and 25 m²/gm. However, values of the mass absorption coefficient above 15 m²/gm are very difficult to explain theoretically. *Quinn et al.* [2003] showed that an internal mixing model could not account for the largest mass absorption coefficient values and *Chuang et al.* [2003] found that relatively complicated black carbon-dust geometries also did not affect the absorption properties significantly (similar to the results of *Fuller et al.* [1999] and *Reimer et al.* [2003]). This relatively large range of mass absorption coefficient results for black carbon is not currently understood and while it has been attributed to difficulties in measuring black carbon mass, to variations in the molecular structure of

black carbon and to complicated particle geometry; the actual causes of the variation remain uncertain. It is apparent, however, that different sources can produce black carbon particles with different mass absorption coefficients.

The average values for the mass absorption coefficients from ACE Asia are actually very similar between investigators. *Clarke et al.* [2003] and *Mader et al.* [2003] report a mean value for the ACE Asia period for mass absorption coefficients of black carbon particles of about $10 \text{ m}^2/\text{gm}$ at 550 nm. *Chuang et al.* [2003] have 12-15 m^2/gm average value at Gosan; $\sim 10 \text{ m}^2/\text{gm}$ for April 12th. *Quinn et al.* [2003] report the mass absorption coefficients for the period considered here was about $12 \text{ m}^2/\text{gm}$.

Mader et al. [2002] measured an aerosol absorption coefficient of 15 Mm^{-1} at 550 nm for April 12th and attributed it all to black carbon deriving a mass absorption coefficient of $27 \text{ m}^2/\text{gm}$. Thus, a power law exponent of 2.0 and a mass absorption coefficient of $27 \text{ m}^2/\text{gm}$ would account for all of the aerosol absorption that we observe since our mass absorption coefficient was 14.7 Mm^{-1} at 550 nm. However, Bond et al. [2002] show that a high mass absorption coefficient correlates with a low power law exponent value. They attribute this behavior to a greater degree of graphitization in the carbon particles that have a high mass absorption coefficient (such as diesel exhaust). Therefore, it appears inconsistent to assume a high mass absorption coefficient and a large power law exponent.

We can attempt to separate out the absorption due to black carbon and the other particles including dust by assuming a range of mass absorption coefficients and a wavelength dependence for the black carbon particles. By subtracting out the black carbon contribution from the total absorption we can estimate the absorption optical depth and single scattering albedo for the remaining, non-black carbon particles.

The results of these calculations for the single scattering albedo are shown in Figure 9. The range of black carbon mass absorption coefficient values used was 10 to $20 \text{ m}^2/\text{gm}$ and the wavelength dependence was assumed to be λ^{-1} . The result is that the single scattering albedo for the non-black carbon particles in Figure 9 is higher than that for the total mixture. The area between the upper curves is shaded to indicate the likely range of possible single scattering albedos for the remaining particles. We have also plotted several other single scattering values for aerosols in the East Asia region for

12/18/03

comparision. The single scattering values from *Li et al.*, [2003] are for Chinese soil particles, *Alfaro et al.*, [2003] from sunphotometer data at the ACE Asia supersite in Zhenbeitai, China for dust events, *Anderson et al.*, [2003] from the PSAP results for the dust cases observed aboard the C130, and *Hoeller et al.*, [2003] is for integrating sphere results for measurements at Yasaka, Japan (see below). The data point labeled SeaWiFS analysis is from the four channel algorithm of *Higurashi and Nakajima* [2002] for April 12th at the Twin Otter location.

4. Thin aerosol layer case: April 16, 2001

The second case that we have examined occurred on April 16, 2001. The optical depth was one of the smallest during the ACE Asia period [*Schmid et al.*, 2003]. On that day the Twin Otter again flew profiles under cloud-free conditions in the Korean Strait. The location of the plane and ship are shown in Figure 10. The Twin Otter was in the same region as it was as on April 12th while the Ron Brown ship was further to the south of Gosan.

4.1 Atmospheric Conditions for April 16, 2001

By April 16th, most of the dust had been removed from the atmosphere and the area became relatively clean. The SeaWiFS image and optical depth analysis for the 16th are shown in Figure 11 a and b. As shown the optical depth was estimated to be quite low (~ 0.1). The flight plan and vertical levels for the Twin Otter are shown in Figure 12. The measured optical depth from the AATS-14 (shown in Figure 13) is in general agreement with the SeaWiFS analysis. The extinction profile shows a layer of aerosol between the surface and about 1 km.

4.2 Measurements of the Spectral Solar Fluxes and Absorption and Estimates of the Spectral Single Scattering Albedo and Absorption Optical depth

The measured and two computed normalized absorption is shown in Figure 14. The fractional absorption is quite low throughout the visible spectrum. The measured value is only slightly above modeled values using a single scattering albedo of 0.99. The estimated single scattering albedo of the aerosol is shown in Figure 15. The single

scattering albedo shows a decrease in the visible (with large error bars) while there is a large amount of scatter in the results past 800 nm. The result from the four channel SeaWiFS analysis of *Higurashi and Nakajima* [2002] for April 16th at the Twin Otter location is also plotted.

While the uncertainty in the measured absorption is larger than the absolute value the derived spectral variation of the single scattering albedo (decreasing with wavelength) shown in Fig 15 is suggestive of absorption by black carbon particles [*Bergstrom et al.*, 2002; 2003; *Dubovik et al.*, 2002; *Eck et al.*, 2002; *Hoeller et al.*, 2003]. Unfortunately, no measurements of black carbon or dust were made on April 16th aboard the Twin Otter so we cannot attempt to estimate the relative amounts of absorption by black carbon and by the other particles. *Chuang et al.* [2003] report black carbon measurements at Gosan on April 16th of approximately $0.8 \mu\text{gm}/\text{m}^3$ and an absorption coefficient of about 6 Mm^{-1} . An EC concentration of $0.5 \mu\text{gm m}^{-3}$ and an absorption coefficient of about 4 Mm^{-1} was measured on the Ron Brown [*Bates et al.*, 2003; *Quinn et al.*, 2003]. In addition, EC made up about 2% of the sub- $10 \mu\text{m}$ aerosol mass of the particles measured on the Ron Brown.

5. Comparison to other aerosol absorption measurements

For the April 12th case our estimated total aerosol absorption coefficient at 550 nm is 14.7 Mm^{-1} that agrees well with *Mader et al.* [2002] who reported 15 Mm^{-1} . On the Ron Brown *Quinn et al.* [2003] measured 12 Mm^{-1} . *Chuang et al.* [2003] report a relatively large value of 27 Mm^{-1} at Gosan, however, it is a 24 hour average. *Quinn et al.* [2003] report a single scattering albedo of 0.94 ± 0.1 for the morning of April 12th. This value is based on measured scattering and absorption coefficients at 55% RH. Using simultaneously measured $f(\text{RH})$ for the scattering coefficient (*Carrico et al.*, 2003), the single scattering albedo was adjusted to ambient RH. This compares to our derived single scattering albedo of 0.90 ± 0.02 at 550 nm.

For April 16th case we estimate an absorption coefficient of 5 Mm^{-1} . On the Ron Brown *Quinn et al.* [2003] measured 4 Mm^{-1} while *Chuang et al.* [2003] measured about 6 Mm^{-1} . For such a small amount of aerosol and the large horizontal variability seen in

12/18/03

ACE Asia (*Anderson et al.*, [2003]; *Redemann et al.*, [2003]), the agreement is fairly good.

As mentioned above, there were a large number of aerosol measurements made during the ACE Asia intensive period. Most of the absorption measurements were made at one wavelength, but *Hoeller et al.* [2003] measured the aerosol single scattering albedo at 450, 550, and 700 nm at Yasaka, Japan during three weeks in March - April 2001. They found that during a dust episode (March 20-23, 2001) the single scattering albedo increased with wavelength while the period with the least amount of dust, the single scattering albedo decreased with wavelength. Their average values at 550 were roughly 0.90 ± 0.05 for the dust period and 0.92 ± 0.01 for the non-dust period. The measurements were not explicitly corrected for relative humidity effects, but the samples were kept at a relative humidity below 35%.

Anderson et al. [2003] made a large number of absorption and scattering measurements on the C-130 during the ACE Asia period. They report mean values of 0.88 ± 0.03 for pollution and 0.96 ± 0.01 for dust single scattering albedo. *Quinn et al.* [2003] observed an average value of 0.93 ± 0.03 at ambient relative humidity (determined as described above) and 550 nm.

6. Summary and Conclusions

Analysis of the solar radiative flux measurements for April 12, 2001 resulted in a single scattering albedo that was 0.8 at 400 nm and increased to 0.95 at about 900 nm and was relatively constant to 1700 nm. Our results and other ACE Asia measurements suggest that the aerosol absorption was due to a mixture of black carbon and mineral dust. We attempted to estimate the amount black carbon absorption by assuming a range of values for the mass absorption coefficient. The absorption then attributed to the remaining particles shows significant UV absorption, but very little visible and near infrared absorption.

The April 16th case was a low optical depth case with very little aerosol. The relative uncertainty is relatively large, but the aerosol appears to be very slightly absorbing. The spectral behavior of the absorption is consistent with black carbon particles from industrial pollution.

Our results imply a relatively complicated aerosol mixture of both industrial pollution (including black carbon) and mineral dust in the ACE Asia region. This underscores the need for careful measurements and analysis to separate out the absorption effects of mineral dust and black carbon in the East Asia region.

7. Acknowledgements

This research was conducted as part of the Asian Pacific Regional Aerosol Characterization Experiment (ACE-Asia). Funding was provided by NASA's Earth Observing System Inter-Disciplinary Science (EOS-IDS) Program, by NASA's Radiation Sciences Program, and by the Aerosol-Climate Interaction Program of NOAA's Office of Global Programs. We would also like to acknowledge the contribution of Professor John Merrill of Rhode Island University in providing his meteorological forecast maps.

8. References

- Anderson, T., S. J. Masonis, D. S. Covert, N. Ahlquist, S. Howell, A. D. Clarke, and C. McNaughton, Variability of aerosol optical properties derived from in situ aircraft measurements during ACE-Asia, *J. Geophys. Res.*, 108(D23), 8647, doi:10.1029/2002JD003247, 2003.
- Bahreini, R., J. L. Jimenez, J. Wang, R. C. Flagan, J. H. Seinfeld, J. Jayne, and D. Worsnop, Aircraft-based aerosol size and composition measurements during ACE-Asia using an aerodyne aerosol mass spectrometer, *J. Geophys. Res.*, 108(D23), 8645, doi:10.1029/2002JD003226, 2003.
- Bates, T.S., P.K. Quinn, D.J. Coffman, D.S. Covert, T.L. Miller, J.E. Johnson, G.R. Carmichael, S.A. Guazzotti, D.A. Sodeman, K.A. Prather, M. Rivera, L.M. Russell, and J.T. Merrill, Marine boundary layer dust and pollution transport associated with the passage of a frontal system over eastern Asian, *J. Geophys. Res.*, *submitted*, 2003.
- Bergstrom, R.W., P.B. Russell and P. Hignett, The wavelength dependence of black carbon particles: Predictions and Results from the TARFOX experiment and Implications for the Aerosol Single Scattering Albedo, *J. Atmos. Sci.*, 59, 567-577, 2002.
- Bergstrom, R., P. Pilewskie, J. Pommier, B. Schmid, P. Russell, Estimates of the spectral aerosol single scattering albedo and aerosol radiative effects during SAFARI 2000, *J. Geophys. Res.*, 108(D13), doi:10.1029/2002JD002435, 2003.

12/18/03

Bond, T.C., Spectral dependence of visible light absorption by carbonaceous particles emitted from coal combustion, *Geophys. Res. Lett.*, 28, 4075-4078, 2001.

Bond, T.C., D.S. Covert, J.C. Kramlich, T.V. Larson, and R.J. Charlson, Primary particle emissions from residential coal burning: optical properties and size distributions, , *J. Geophys. Res.*, 107(D21), 8347, doi:10.1029/2001JD000571, 2001, 2002.

Bush, B. C., and F. Valero, Surface aerosol radiative forcing at Gosan during the ACE-Asia Campaign, *J. Geophys. Res.*, 108(D23), 8660, doi:10.1029/2002JD003233, 2003.

Carrico, C., P. Kus, M. Rood, P. Quinn, and T. Bates, Mixtures of pollution, dust, seasalt, and volcanic aerosol during ACE-Asia: Aerosol radiative properties as a function of relative humidity, *J. Geophys. Res.*, 108(D23), 8650, doi:10.1029/2003JD0033405, 2003.

Chandrasekhar, *Radiative Transfer*, McGraw-Hill, New York, 393 pg, (1960).

Chin, M., P. Ginoux, R. Lucchesi, B. Huebert, R. Weber, T. Anderson, S. Masonis, B. Blomquist, A. Bandy, and D. Thornton, A global aerosol model forecast for the ACE-Asia field experiment, *J. Geophys. Res.*, 108(D23), 8654, doi:10.1029/2003JD003642, 2003.

Chuang, P. Y., R. Duvall, M. Bae, A. Jefferson, J. Schauer, H. Yang, J. Yu, and J. Kim, Observations of elemental carbon and absorption during ACE-Asia and implications for aerosol radiative properties and climate forcing, *J. Geophys. Res.*, 108(D23), 8634, doi:10.1029/2002JD003254, 2003.

Conant, W. C., J. H. Seinfeld, J. Wang, G. R. Carmichael, Y. Tang, I. Uno, P. J. Flatau, K. M. Markowicz, and P. K. Quinn, A model for the radiative forcing during ACE-Asia derived from CIRPAS Twin Otter and R/V Ronald H. Brown data and comparison with observations, *J. Geophys. Res.*, 108(D23), 8661, doi:10.1029/2002JD003260, 2003.

Dubovik, O., B.N. Holben, Y.J. Kaufman, M. Yamasoe, A. Smirnov, D. Tanre, and I. Slutsker, Single scattering albedo of smoke retrieved from the sky radiance and solar transmittance measured from ground, *J Geophys Res*, Vol 103, 31903-31,923, (1998)

Dubovik, O., B. Holben, T.F. Eck, A. Smirnov, Y. Kaufman, M.D. King, D. Tanre, I. Slutsker, Variability of Absorption and Optical Properties of Key Aerosol Types Observed in Worldwide Locations, *J. Atmos. Sci*, 59, 590-608, (2002).

Eck T.F., and others, Variability of biomass burning aerosol optical characteristics in southern Africa during SAFARI 2000 dry season campaign and a comparison of single scattering albedo estimates from radiometric measurements *J. Geophys. Res.*, submitted, (2002).

Eck, T.F., B.N. Holben, D.E. Ward, O. Dubovik, J.S. Reid, A. Smirnov, M.M Mukelabai, N.C. Hsu, N.T. O'Neil, and I. Slutsker, Characterization of the optical properties of

12/18/03

biomass burning aerosol in Zambia during the 1997 ZIBBEE field campaign, *J. Geophys. Res.*, 106 3425-3448, (2001).

Fuller, K.A., W.C. Malm and S.M. Kreidenweis, Effects of mixing on extinction by carbonaceous particles, *J. Geophys. Res.*, 15,941-15,954, (1999)

Higurashi, A., and T. Nakajima, 2002: Detection of aerosol types over the East China Sea near Japan from four-channel satellite data. *Geophys. Res. Lett.*, 29(17), 1836, doi:10.1029/2002GL015357

Höller, R., K. Ito, S. Tohno, and M. Kasahara, Wavelength-dependent aerosol single-scattering albedo: Measurements and model calculations for a coastal site near the Sea of Japan during ACE-Asia, *J. Geophys. Res.*, 108(D23), 8648, doi:10.1029/2002JD003250, 2003.

Huebert, B. J., T. Bates, P. B. Russell, G. Shi, Y. J. Kim, K. Kawamura, G. Carmichael, and T. Nakajima, An overview of ACE-Asia: Strategies for quantifying the relationships between Asian aerosols and their climatic impacts, *J. Geophys. Res.*, 108(D23), 8633, doi:10.1029/2003JD003550, in press, 2003.

Huebert, B.J., T. Bates, P.B. Russell, G. Shi, Y.J. Kim, K. Kawamura, G. Carmichael and T. Nakajima, An overview of ACE-Asia: Technical Appendix, accepted, *J. Geophys. Res.*, 2003b.

Jacob, D.J., J.H. Crawford, M.M. Kleb, V.E. Connors, R.J. Bendura, J.L. Raper, G.W. Sachse, J.C. Gille, and L. Emmons, The Transport and Chemical Evolution over the Pacific (TRACE-P) Mission: design, execution, and overview of first results, *J. Geophys. Res.*, *In press*, 2003.

Jaffe, D., I. McKendry, T. Anderson, and H. Price, Six 'New' Episodes of Trans-Pacific Transport of Air Pollutants, *Atmos. Environ.*, 37, 391,2003 [or The April 2001 Asian dust events: Transport and substantial impact on surface particulate matter concentrations across the United States *By Dan Jaffe, Julie Snow and Owen Cooper EOS, In-press, June 2003*]

Kim, Y. S., et al., Dust particles in the free atmosphere over desert areas on the Asian continent: Measurements from summer 2001 to summer 2002 with balloon-borne optical particle counter and lidar, Dunhuang, China, *J. Geophys. Res.*, 108(D23), 8643, doi:10.1029/2002JD003269, in press, 2003.

Kline, J.T., Huebert, B.J., Howell, S.G. Uematsu, M. and H. Tsurata, Parameters for Modeling Aerosol Absorption: Measurements in Biomass Burning Smoke, Urban/Industrial Plumes, and NW Pacific Marine Airmasses, Abstract A22-F-07, AGU Fall Meeting, San Francisco, CA, (2003)

Kurucz, R.L., Synthetic infrared spectra, in *Infrared Solar Physics*, IAU Symp, 154, edited by D.M. Rabin and J.T. Jeffries, Kluwer Acad., Norwell, MA, (1992). (Available on the LBLRTM web site)

Li, L., H. Fukushima, R. Fruin, B. G. Mitchell, M. He, I. Uno, T. Takamura and S. Ohta, Influence of submicron absorptive aerosol on SeaWiFS derived marine reflectance during ACE - Asia, *J. Geophys. Res.*, 108(D15), 4472, doi:10.1029/2002JD002776, 2003.

Liu, M., D. L. Westphal, S. Wang, A. Shimizu, N. Sugimoto, J. Zhou, and Y. Chen, A high-resolution numerical study of the Asian dust storms of April 2001, *J. Geophys. Res.*, 108(D23), 8653, doi:10.1029/2002JD003178, 2003.

Mader, B. T., R. C. Flagan, and J. H. Seinfeld, Airborne measurements of atmospheric carbonaceous aerosols during ACE-Asia, *J. Geophys. Res.*, 107(D23), 4704, doi:10.1029/2002JD002221, 2002.

Markowicz, K. M., P. J. Flatau, P. K. Quinn, C. M. Carrico, M. K. Flatau, A. M. Vogelmann, D. Bates, M. Liu, and M. J. Rood, Influence of relative humidity on aerosol radiative forcing: An ACE-Asia experiment perspective, *J. Geophys. Res.*, 108(D23), 8662, doi:10.1029/2002JD003066, 2003.

Matsuki, A., et al., Seasonal dependence of the long-range transport and vertical distribution of free tropospheric aerosols over East Asia: On the basis of aircraft and lidar measurements, and isentropic trajectory analysis, *J. Geophys. Res.*, 108(D23), 8663, doi:10.1029/2002JD003266, 2003.

Matsumoto, K., M. Uematsu, T. Hayano, K. Yoskioka, H. Tanimoto, and T. Iida, Simultaneous measurements of particulate elemental carbon on the ground observation network over the western North Pacific during the ACE-Asia campaign, *J. Geophys. Res.*, 108(D23), 8635, doi:10.1029/2002JD002744, 2003a.

Matsumoto, K., Y. Uyama, T. Hayano, H. Tanimoto, I. Uno, and M. Uematsu, Chemical properties and outflow patterns of anthropogenic and dust particles on Rishiri Island during the Asian Pacific Regional Aerosol Characterization Experiment (ACE-Asia), *J. Geophys. Res.*, 108(D23), 8666, doi:10.1029/2003JD003426, 2003b.

Mlawer, E.J., S.J. Taubman, P.D. Brown, M.J. Iacono and S.A. Clough Radiative Transfer for Inhomogeneous Atmospheres: RRTM, a Validated correlated-k model for the longwave. *J. Geophys. Res.*, 102, 4353-4356, (1997).

Murayama, T., et al., An intercomparison of lidar-derived aerosol optical properties with airborne measurements near Tokyo during ACE-Asia, *J. Geophys. Res.*, 108(D23), 8651, doi:10.1029/2002JD003259, 2003.

Nakajima, T. et al., Significance of direct and indirect radiative forcing of aerosols in the East China Sea region, *J. Geophys. Res.*, in press (2003).

12/18/03

Osada, K., M. Kido, H. Iida, K. Matsunaga, Y. Iwasaka, M. Nagatani, and H. Nakada, Seasonal variation of free tropospheric aerosol particles at Mt. Tateyama, central Japan, *J. Geophys. Res.*, 108(D23), 8667, doi:10.1029/2003JD003544, 2003.

Pilewskie, P.; Pommier, J.; Bergstrom, R.; Gore, W.; Howard, S.; Rabbette, M.; Schmid, B.; Hobbs, P. V.; Tsay, S. C. Solar spectral radiative forcing during the Southern African Regional Science Initiative J. Geophys. Res. Vol. 108 No. D13 10.1029/2002JD002411 13 March 2003.

Quinn, P.K., D.J. Coffman, T.S. Bates, E.J. Welton, D.S. Covert, T.L. Miller, J.E. Johnson, S. Maria, L. Russell, R. Arimoto, C.M. Carrico, M.J. Rood, and J. Anderson, Aerosol Optical Properties Measured Onboard the *Ronald H. Brown* During ACE Asia as a Function of Aerosol Chemical Composition and Source Region, *J. Geophys. Res.*, submitted, 2003.

Redemann, J., S. J. Masonis, B. Schmid, T. L. Anderson, P. B. Russell, J. M. Livingston, O. Dubovik, and A. D. Clarke, Clear-column closure studies of aerosols and water vapor aboard the NCAR C-130 during ACE-Asia, 2001, *J. Geophys. Res.*, 108(D23), 8655, doi:10.1029/2003JD003442, in press, 2003.

Reimer, N., H. Vogel, B. Vogel and F. Fiedler, Modeling aerosols on the mesoscale- γ : Treatment of soot aerosol and its radiative effects, *J. Geophys. Res.*, 108(D19), 4601, doi:10.1029/2003JD003448, 2003.

Sano, I., S. Mukai, Y. Okada, B. N. Holben, S. Ohta, and T. Takamura, Optical properties of aerosols during APEX and ACE-Asia experiments, *J. Geophys. Res.*, 108(D23), 8649, doi:10.1029/2002JD003263, 2003.

Schnaiter et al, UV-VIS-NIR spectral optical properties of soot and soot-containing aerosols, *J. Aerosol Science*, 34, 1421-1444, (2003).

Schmid, B., et al., Column closure studies of lower tropospheric aerosol and water vapor during ACE-Asia using airborne Sun photometer and airborne in situ and ship-based lidar measurements, *J. Geophys. Res.*, 108(D23), 8656, doi:10.1029/2002JD003361, 2003.

Sokolik I.N. and O.B. Toon. Incorporation of mineralogical composition into models of the radiative properties of mineral aerosol from UV to IR wavelengths. *J. Geophys. Res.*, 104, 9423-9444, 1999.

Stamnes, K., S.-C. Tsay, W. Wiscombe and K. Jayaweera, A numerically stable algorithm for discrete-ordinate-method radiative transfer in multiple scattering and emitting layered media, *Appl. Opt.* 27, 2502-2509, (1988).

Takemura, T., T. Nakajima, A. Higurashi, S. Ohta, and N. Sugimoto, Aerosol distributions and radiative forcing over the Asian Pacific region simulated by Spectral

12/18/03

Radiation-Transport Model for Aerosol Species (SPRINTARS), *J. Geophys. Res.*, 108(D23), 8659, doi:10.1029/2002JD003210, 2003.

Thulasiraman, S., N. T. O'Neill, A. Royer, B. N. Holben, D. L. Westphal, and L. J. B. McArthur. Sunphotometric observations of the 2001 Asian dust storm over Canada and the U.S. *Geophys. Res. Lett.* 10.1029/2001GL014188, 2002

Uno, I., et al., Regional chemical weather forecasting system CFORS: Model descriptions and analysis of surface observations at Japanese island stations during the ACE-Asia experiment, *J. Geophys. Res.*, 108(D23), 8668, doi:10.1029/2002JD002845, 2003.

Uno, I., G. R. Carmichael, D. Streets, S. Satake, T. Takemura, J.-H. Woo, M. Uematsu, and S. Ohta, Analysis of surface black carbon distributions during ACE-Asia using a regional-scale aerosol model, *J. Geophys. Res.*, 108(D23), 8636, doi:10.1029/2002JD003252, 2003.

Wang, J., et al., Clear-column radiative closure during ACE-Asia: Comparison of multiwavelength extinction derived from particle size and composition with results from Sun photometry, *J. Geophys. Res.*, 107(D23), 4688, doi:10.1029/2002JD002465, 2002.

Wang, J., S. A. Christopher, F. J. Brechtel, J. Kim, B. Schmid, J. Redemann, P. B. Russell, P. K. Quinn, and B. Holdben, Geostationary satellite retrievals of aerosol optical thickness during ACE-Asia, *J. Geophys. Res.*, 108(D23), 8657, doi:10.1029/2003JD003580, in press, 2003.

8. List of Figures

Figure 1: Measured and calculated downward flux at 2 km above the surface on April 12, 2001.

Figure 2 - Location of the Ron Brown, the Twin Otter and the C-130 on April 12, 2001

Figure 3: a) SeaWiFS RGB color image on April 12, 2001
b) Aerosol Optical depth map

Figure 4: Twin Otter flight tracks on April 12, 2001

Figure 5: Vertical profiles of aerosol optical depth and extinction coefficient from the AATS-14 aboard the Twin Otter for April 12, 2001

Figure 6: Measured and calculated fractional absorption for April 12, 2001

Figure 7: Figure 7 - Derived aerosol single scattering albedo. The smooth curve is a fit to the results.

Figure 8: Wavelength dependence of aerosol optical depth and derived aerosol absorption optical depth

Figure 9: Figure 9 Estimated range of single scattering albedo for mixture and for the non-black carbon particles

Figure 10 - Location of the Ron Brown, Twin Otter and C-130 for April 16th

Figure 11: a) SeaWiFS RGB color image on April 16, 2001
b) Aerosol Optical depth map

Figure 12: Twin Otter flight tracks on April 16, 2001

Figure 13: Aerosol optical depth and extinction coefficient from the AATS-14 aboard The Twin Otter for April 16, 2001

Figure 14: Measured and calculated fractional absorption for April 16, 2001

Figure 15 - Estimated aerosol single scattering albedo; solid line is a fit to the results

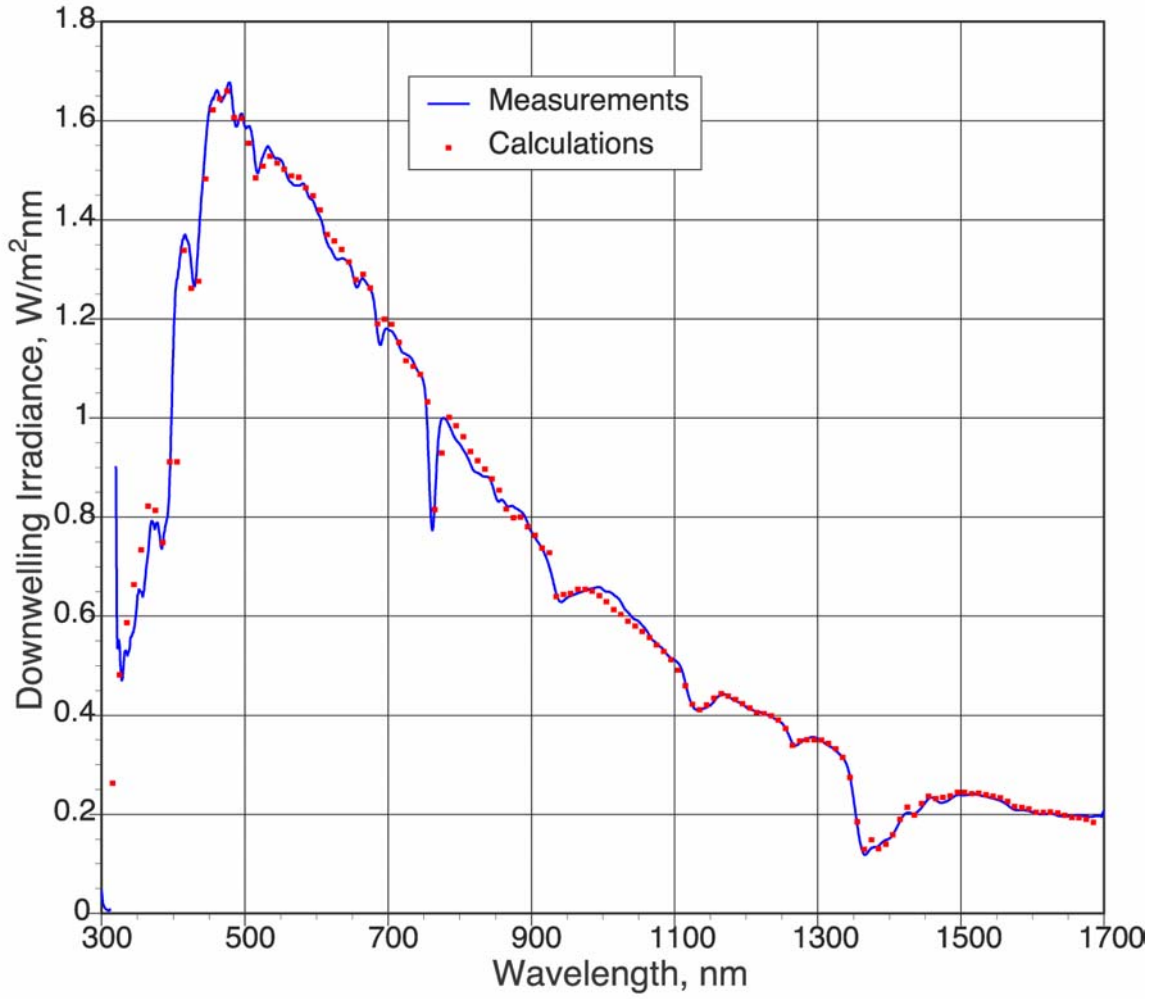


Figure 1 Measured and calculated downward flux at 2 km above the surface on April 12, 2001.

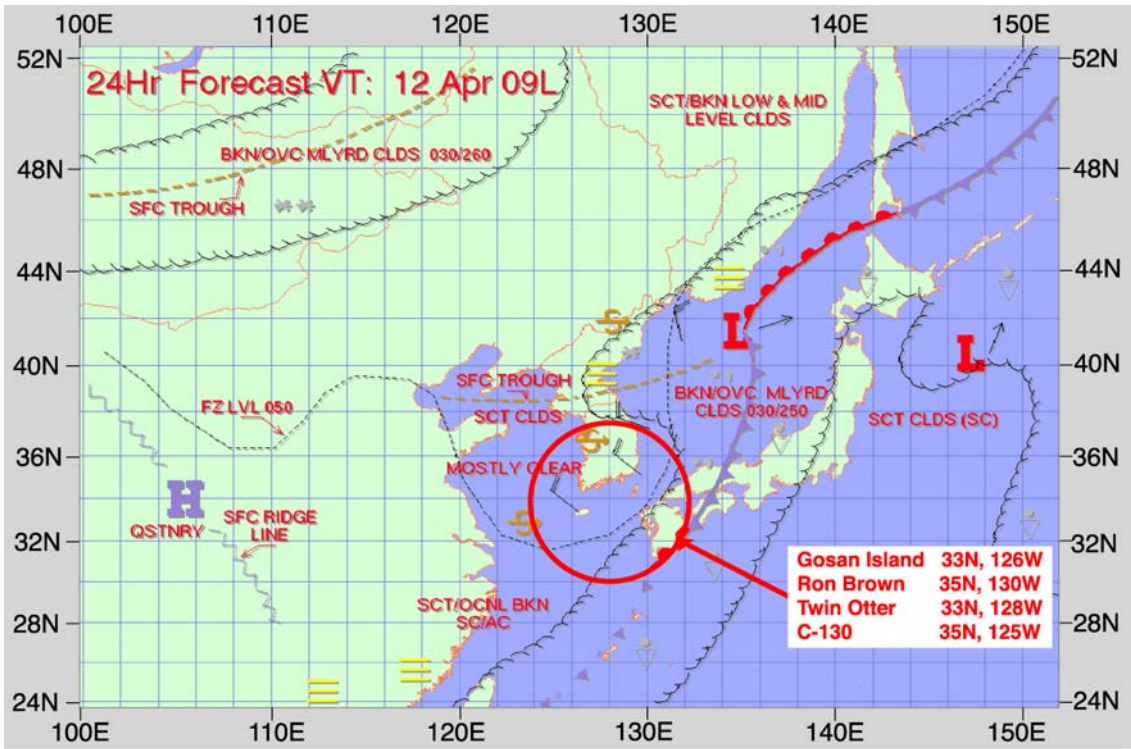


Figure 2 Location of the Ron Brown, the Twin Otter and the C-130 on April 12, 2001.

12/18/03

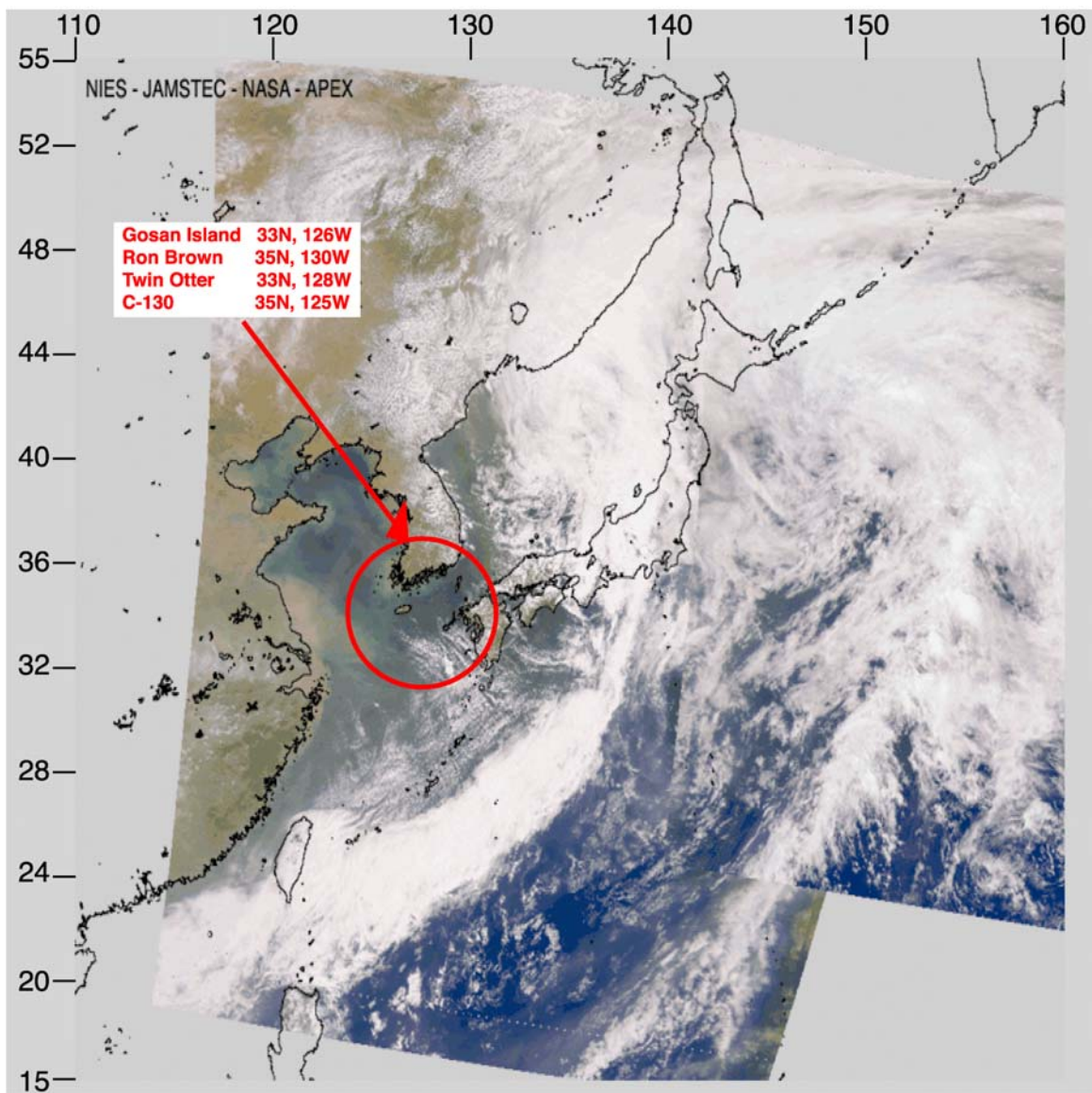


Figure 3a an RGB (natural color) SeaWiFS image for April 12, 2001.

12/18/03

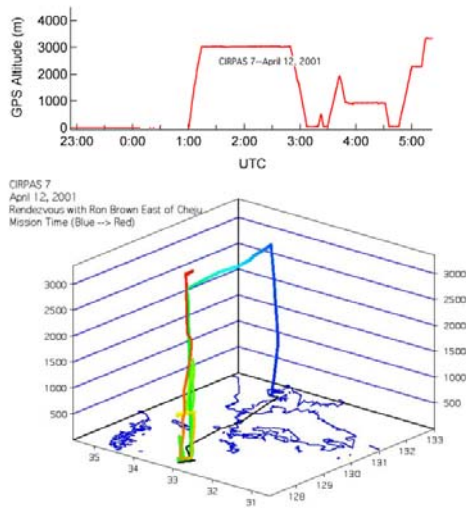


Figure 4 Twin Otter location and altitude for April 12, 2001.

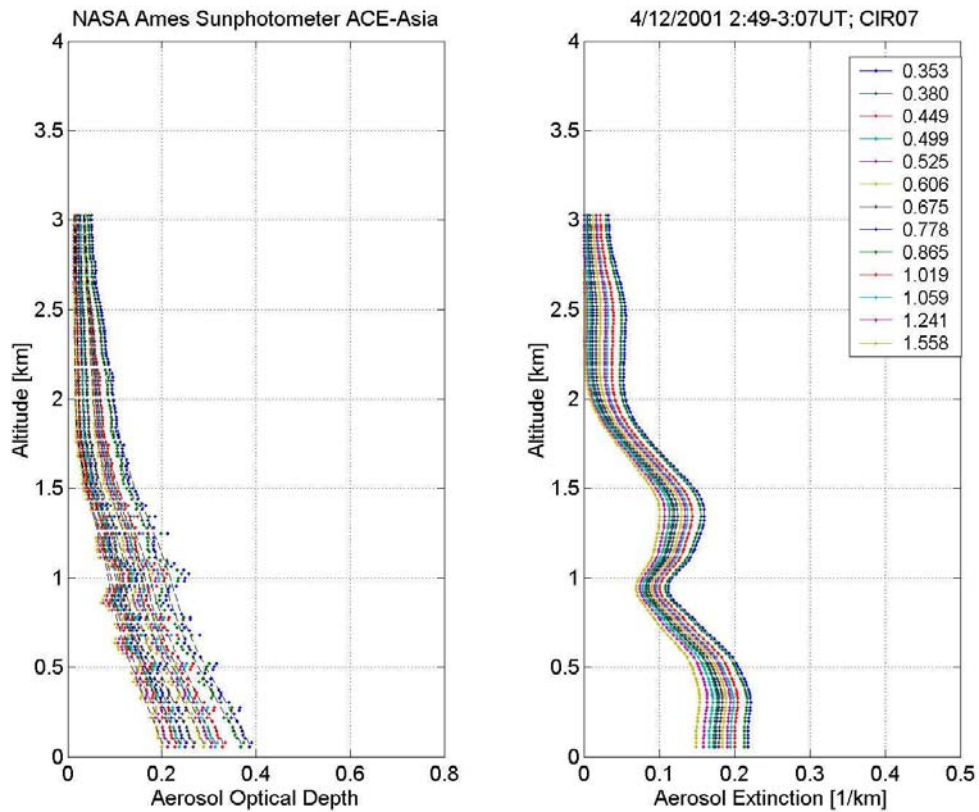


Figure 5 Vertical profiles of aerosol optical depth and extinction coefficient from the AATS-14 aboard the Twin Otter for April 12, 2001

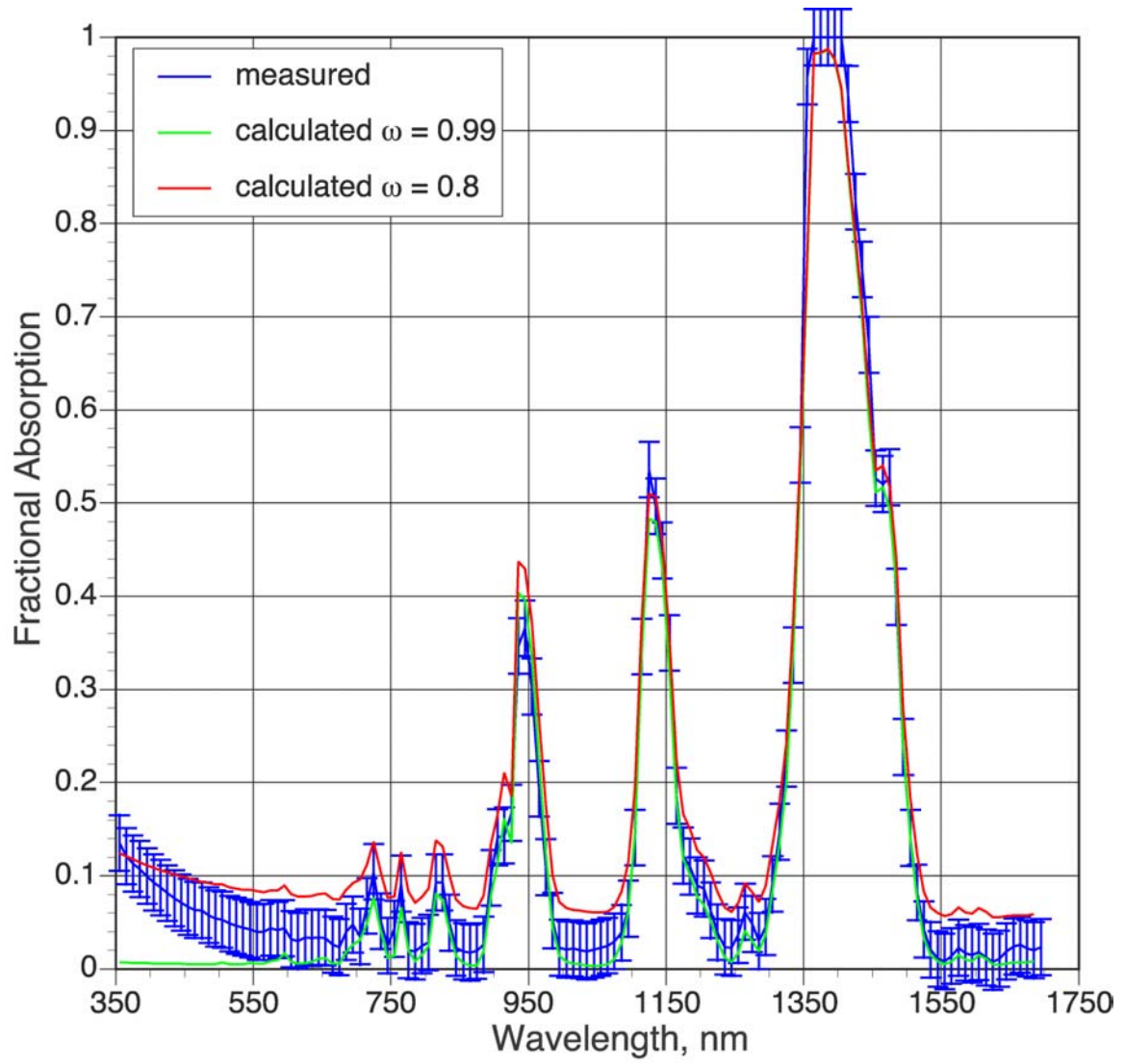


Figure 6 April 12th measured and calculated fractional absorption

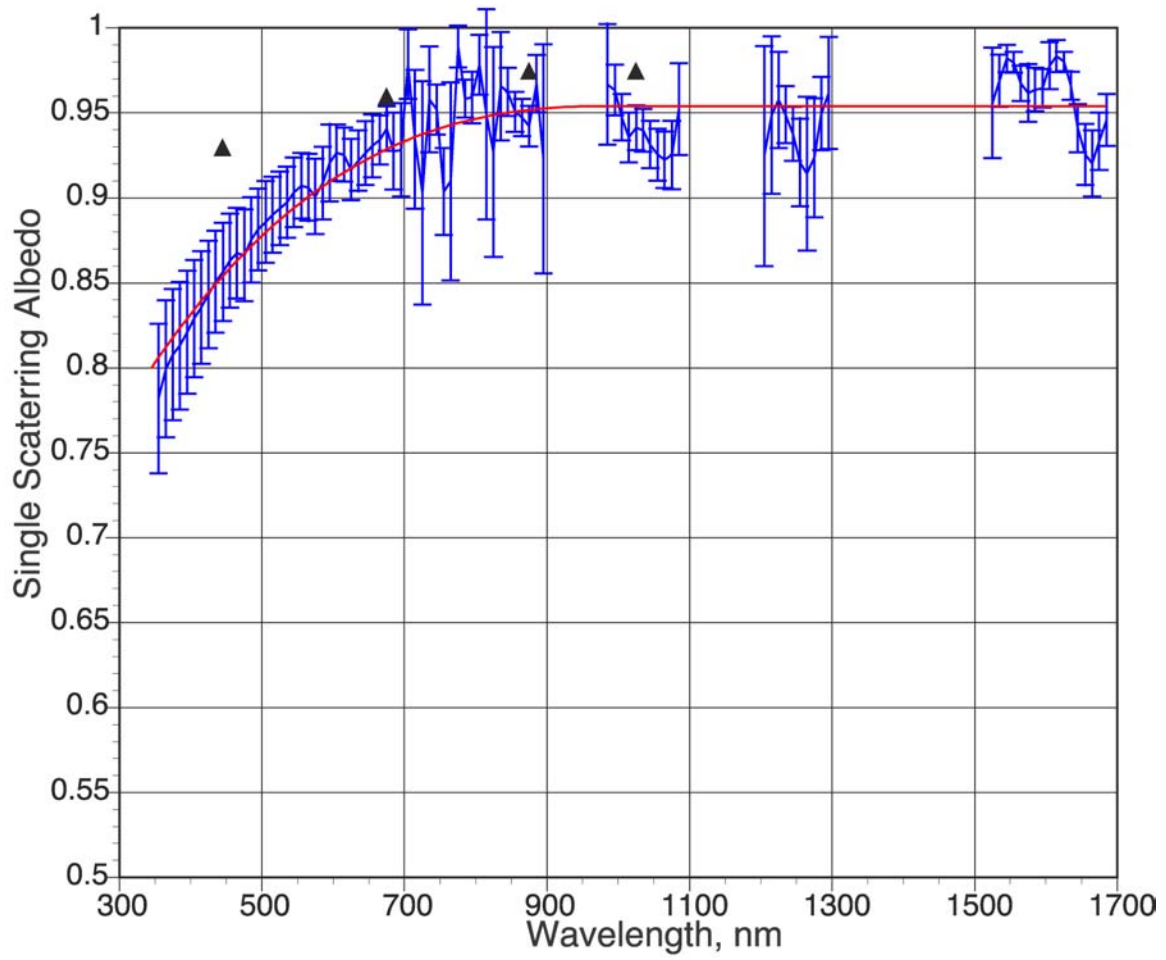


Figure 7 Derived aerosol single scattering albedo. The smooth curve is a fit to the results. ▲ Persian Gulf Dust; Dubovik et al., (2002).

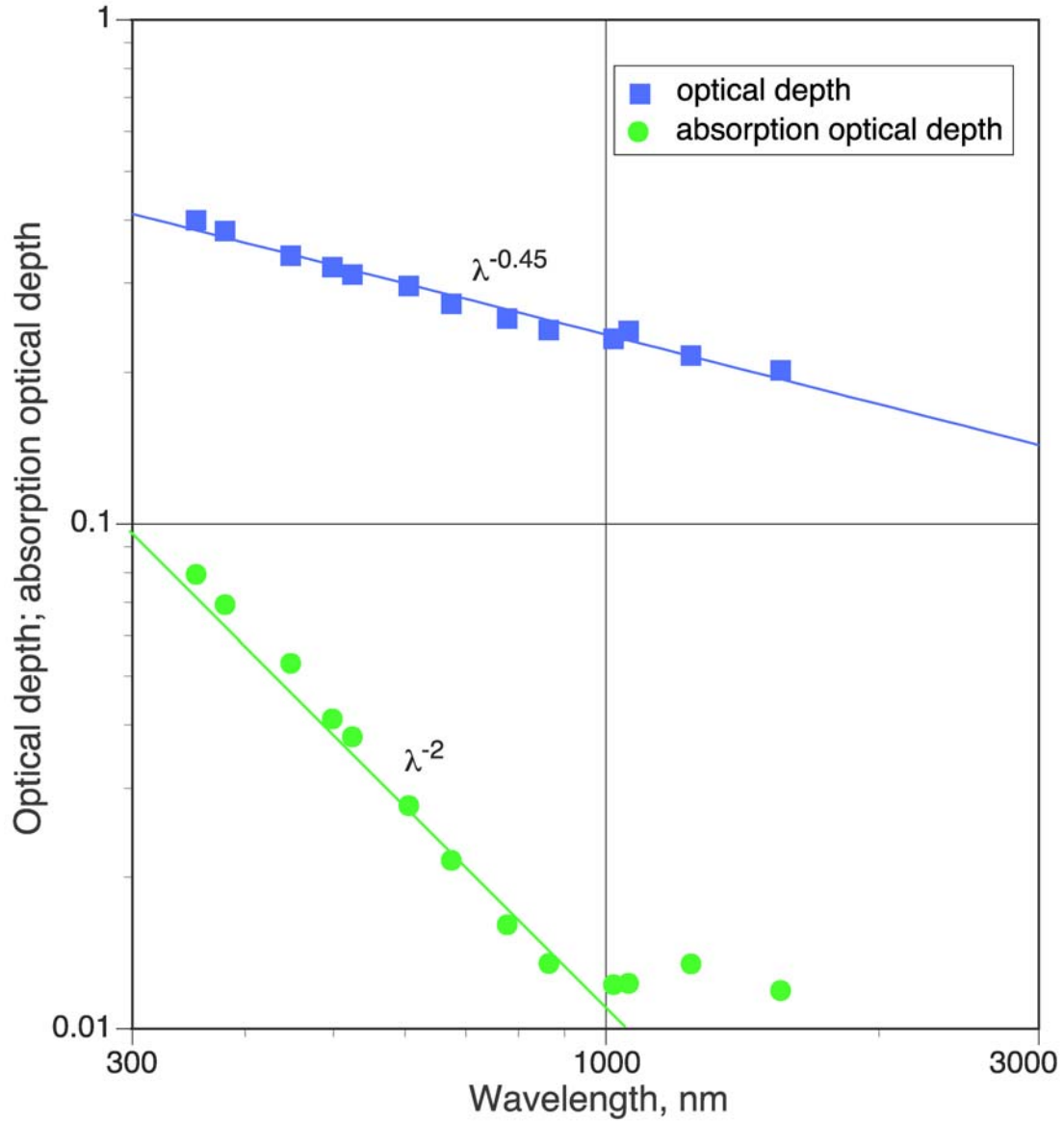


Figure 8 Wavelength dependence of aerosol optical depth and derived aerosol absorption optical depth.

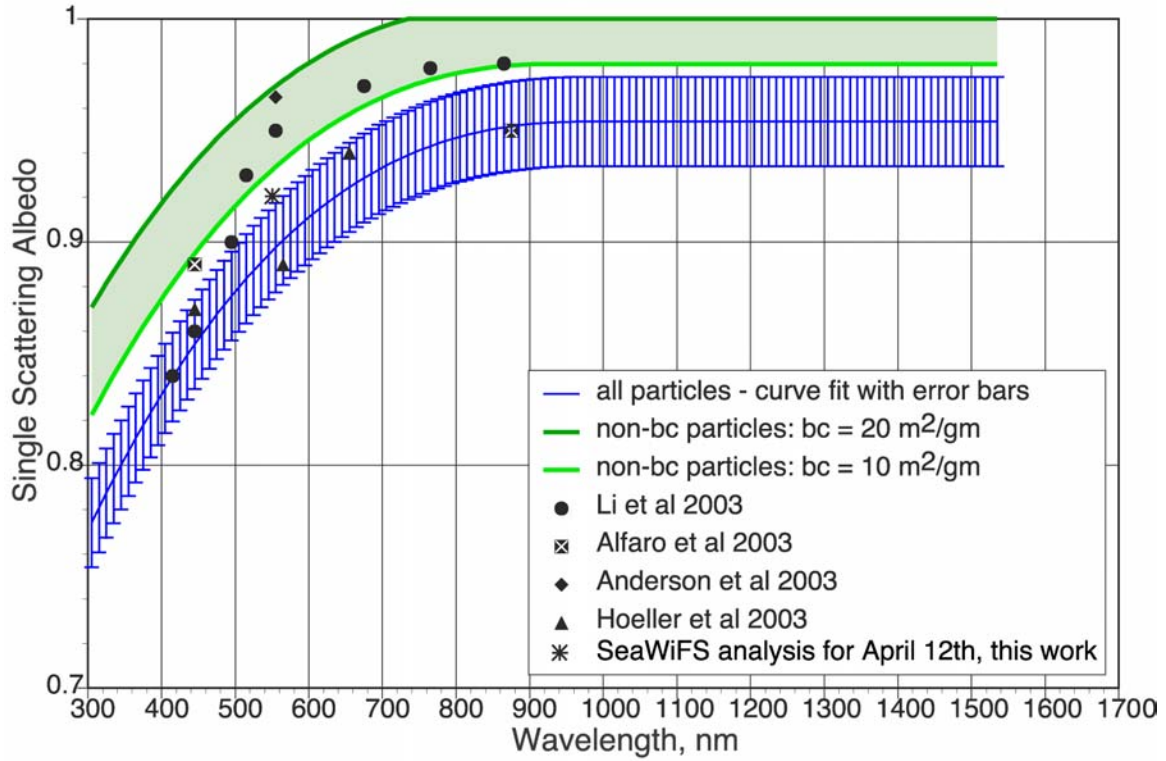


Figure 9 Estimated range of single scattering albedo for mixture and for the non-black carbon particles.

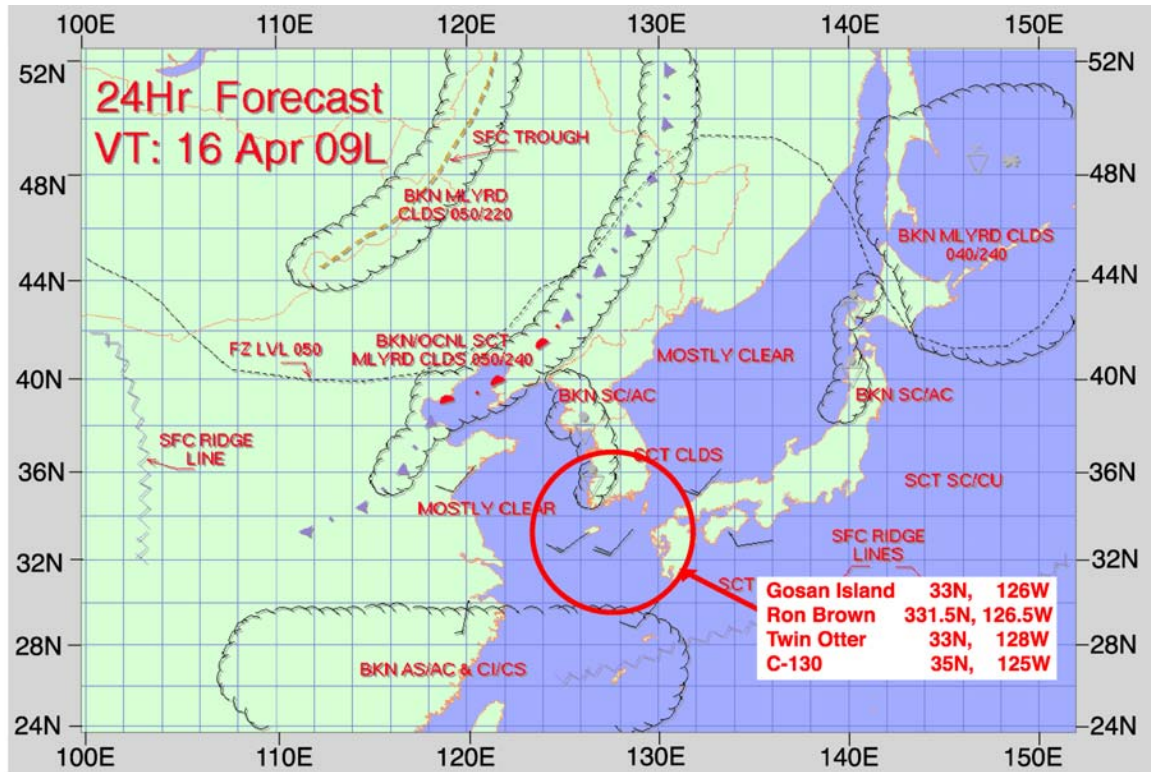


Figure 10 Location of the Ron Brown, the Twin Otter and C-130 for April 16, 2001.

12/18/03

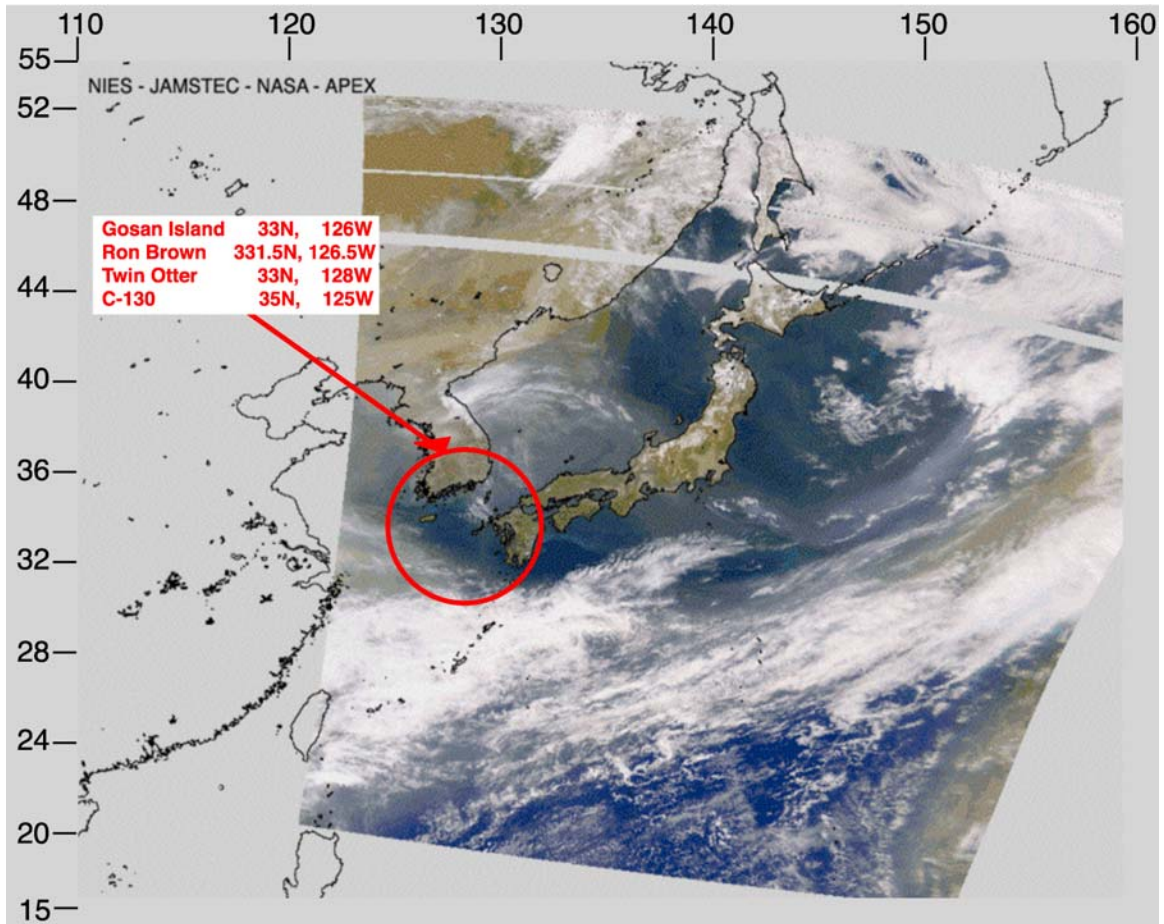


Figure 11a SeaWiFS image for April 16, 2001.

12/18/03

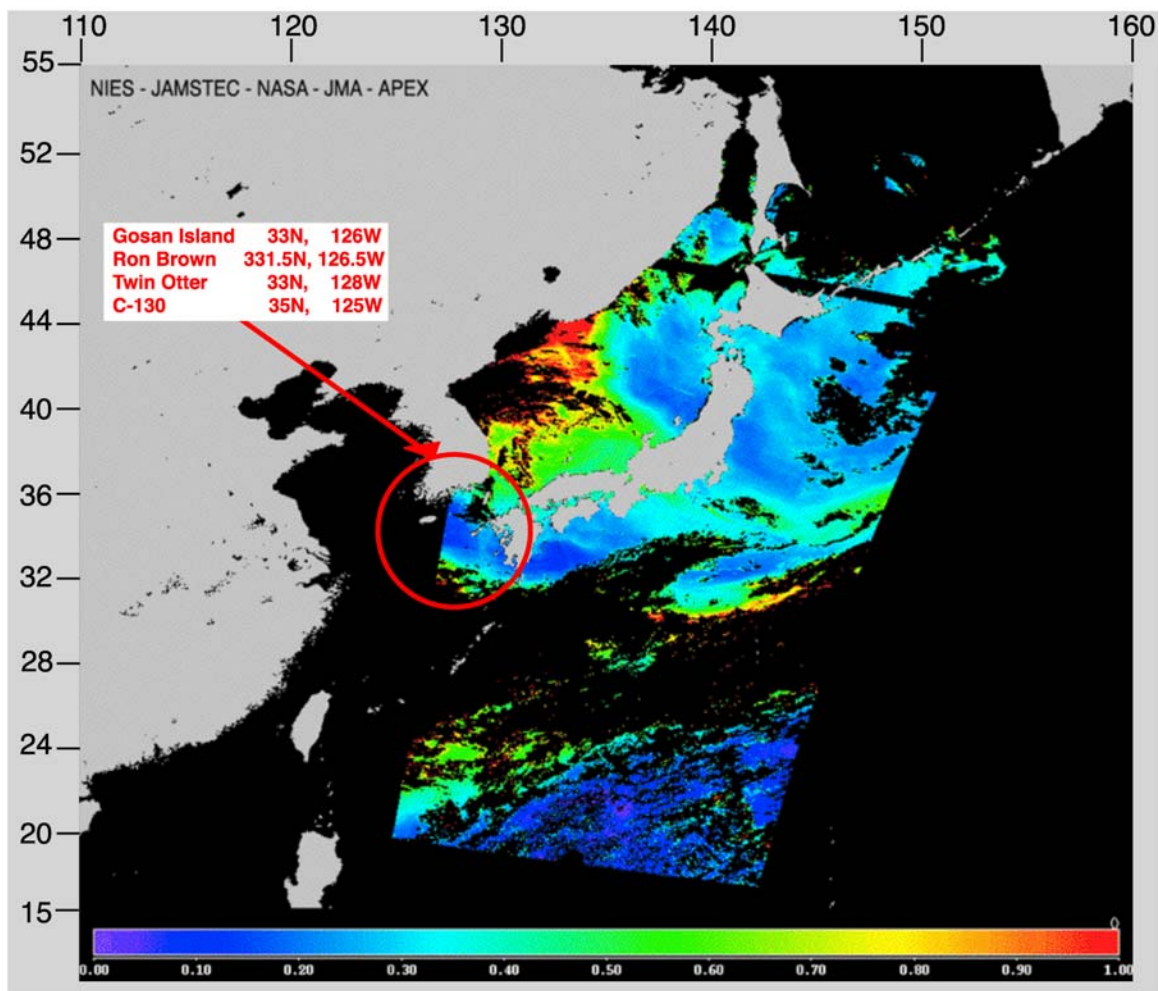


Figure 11b Optical depth map from the SeaWiFS analysis for April 16, 2001.

12/18/03

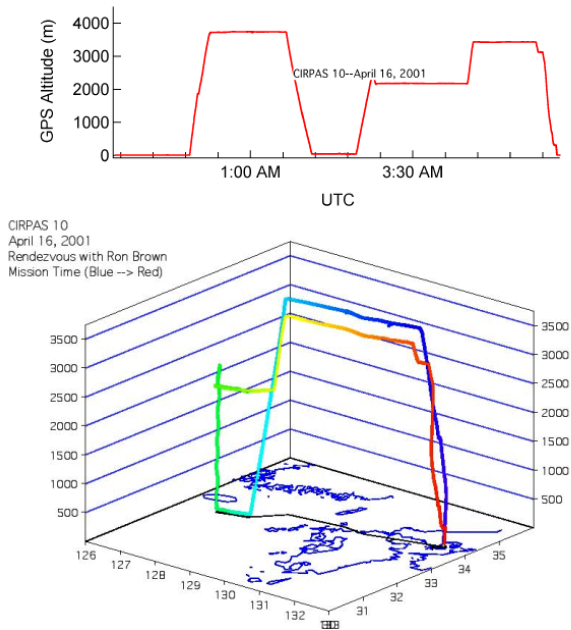


Figure 12 Flight path of the Twin Otter for April 16, 2001

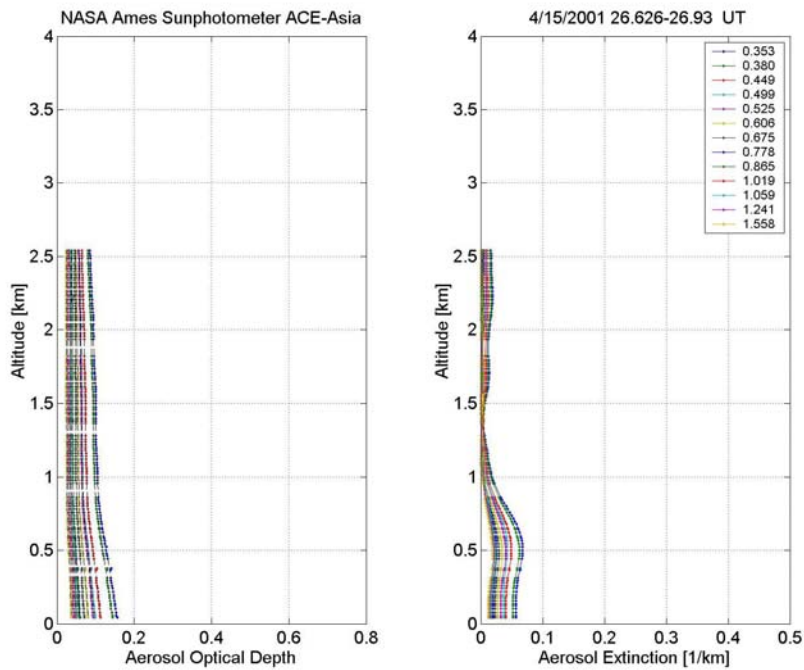


Figure 13 Aerosol optical depth and extinction coefficient from the AATS-14 aboard The Twin Otter for April 16, 2001

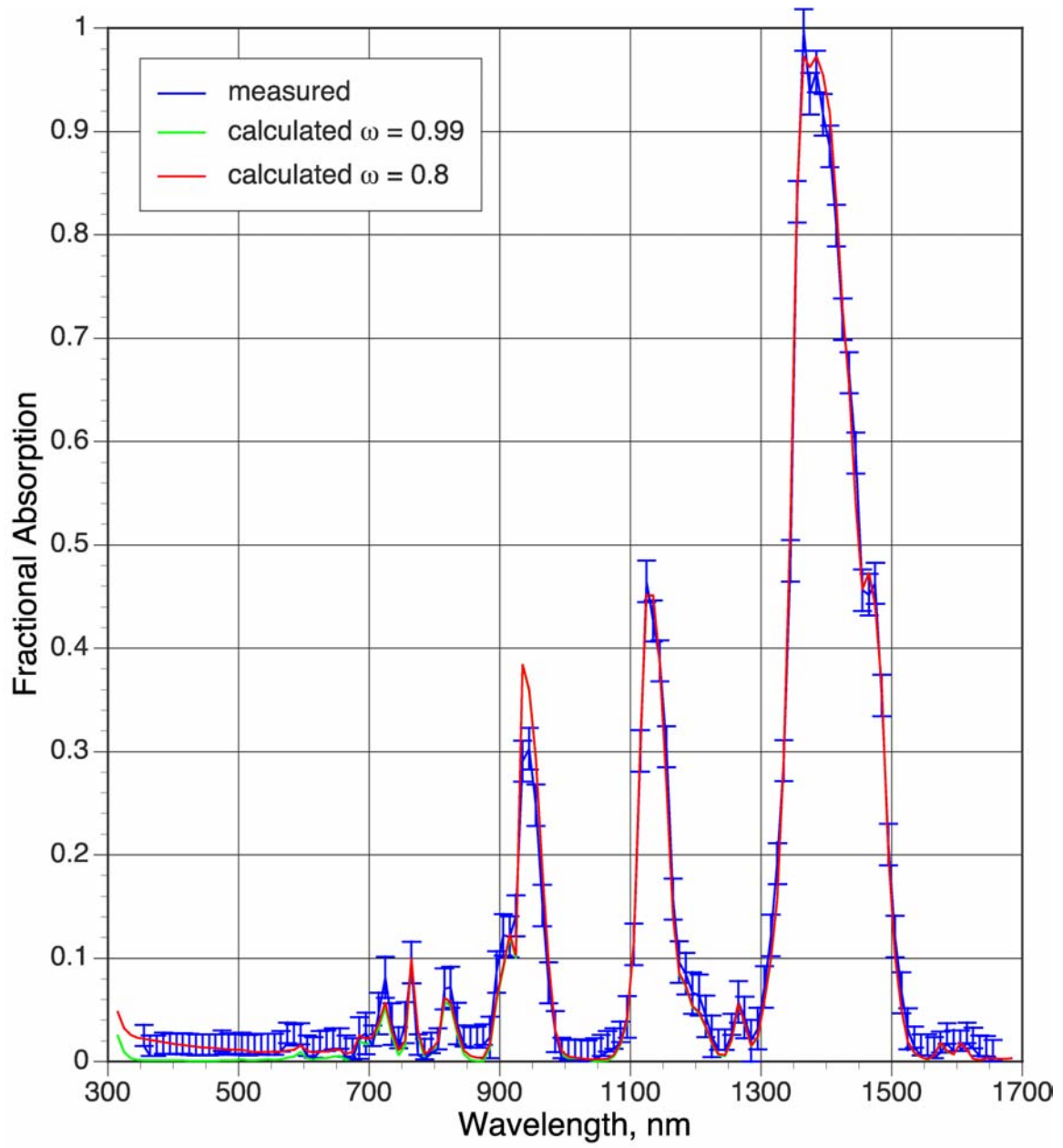


Figure 14 April 16th measured and calculated fractional absorption.

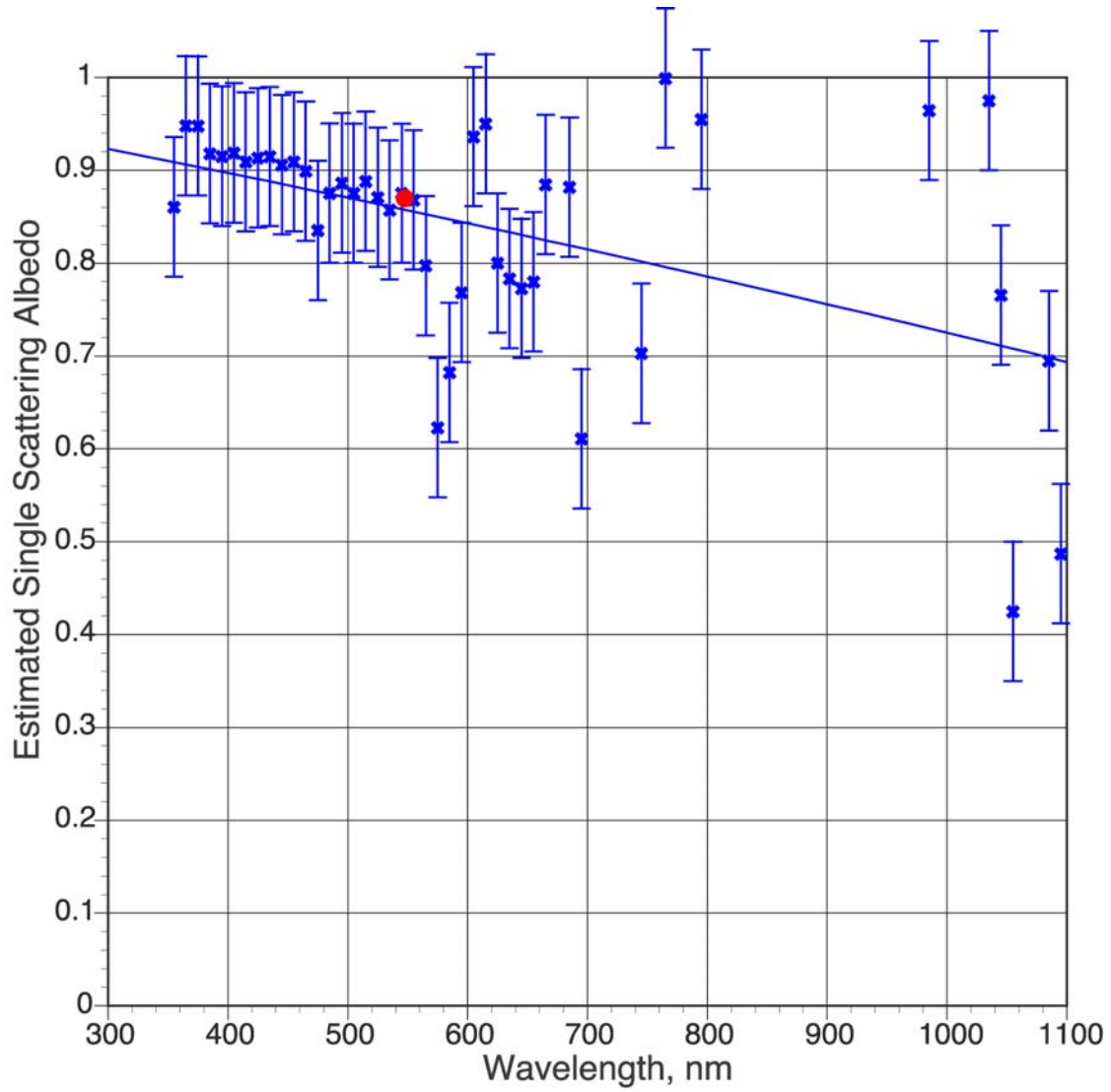


Figure 15 Estimated aerosol single scattering albedo; solid line is a fit to the results; ● is SeaWiFS analysis for April 16th, this work.